Carbohydrate Polymers 117 (2015) 422–433

Contents lists available at ScienceDirect

Carbohydrate Polymers

journal homepage: www.elsevier.com/locate/carbpol

Study on *Dendrobium officinale* *O*-acetyl-glucomannan (Dendronan®): Part II. Fine structures of *O*-acetylated residues

Xiaohui Xing[a,b], Steve W. Cui[b,*], Shaoping Nie[c], Glyn O. Phillips[d,e], H. Douglas Goff[a], Qi Wang[b]

[a] *Department of Food Science, University of Guelph, Guelph, ON, Canada N1G 2W1*
[b] *Guelph Food Research Centre, Agriculture and Agri-Food Canada, Guelph, ON, Canada N1G 5C9*
[c] *State Key Laboratory of Food Science and Technology, Nanchang University, Nanchang 330047, Jiangxi, China*
[d] *Glyn O. Phillips Hydrocolloid Research Centre, Glyndŵr University, Wrexham LL11 2AW, UK*
[e] *Phillips Hydrocolloids Research Ltd., 45 Old Bond Street, London W1S 4QT, UK*

ARTICLE INFO

Article history:
Received 21 May 2014
Received in revised form 6 August 2014
Accepted 7 August 2014
Available online 23 September 2014

Keywords:
Detailed structure
Dendrobium officinale
Glucomannan
NMR
Mannanase
2,3-Di-*O*-acetyl-β-D-mannopyranose

ABSTRACT

Main objective of this study was to investigate the detailed structural information about *O*-acetylated sugar residues in Dendronan®. A water solution (2%, w/w) of Dendronan® was treated with endo-β-mannanase to produce oligosaccharides rich in *O*-acetylated sugar residues. The oligosaccharides were partly recovered by ethanol precipitation (70%, w/w). The recovered sample (designated Hydrolyzed *Dendrobium officinale* Polysaccharide, HDOP) had a yield of 24.7% based on the dry weight of Dendronan® and was highly *O*-acetylated. A D_2O solution of HDOP (6%, w/w) generated strong signals in ^1H, ^{13}C, 2D ^1H–^1H COSY, 2D ^1H–^1H TOCSY, 2D ^1H–^1H NOESY, 2D ^1H–^{13}C HMQC, and 2D ^1H–^{13}C HMBC NMR spectra. Results of NMR analyses showed that the majority of *O*-acetylated mannoses were mono-substituted with acetyl groups at O-2 or O-3 position. There were small amounts of mannose residues with di-*O*-acetyl substitution at both O-2 and O-3 positions. Minor levels of mannoses with 6-*O*-acetyl, 2,6-di-*O*-acetyl, and 3,6-di-*O*-acetyl substitutions were also identified. Much information about sugar residue sequence was extracted from 2D ^1H–^{13}C HMBC and 2D ^1H–^1H NOESY spectra. $^1J_{C-H}$ coupling constants of major sugar residues were obtained. Evidences for the existence of branches or *O*-acetylated glucoses in HDOP were not found. The major structure of Dendronan® is shown as follows:

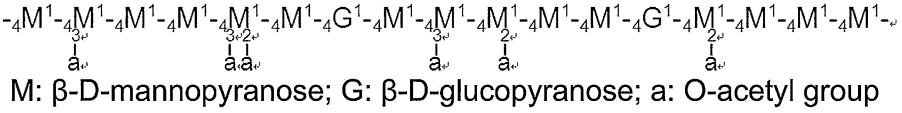

M: β-D-mannopyranose; G: β-D-glucopyranose; a: O-acetyl group

1. Introduction

Dendrobium officinale plant is an important traditional Chinese herbal medicine and nutraceutical food with many health-enhancing functions (Hua, Zhang, Fu, Chen, & Chan, 2004). The demand for this particular food is so high that more than 130 companies are producing it for commercial purposes in China. Because of the importance of the plant, it is meaningful to understand its chemical components. Previously, we successfully isolated Dendronan®, an 2,3-*O*-acetyl-glucomannan, from dry *D. officinale* herbal samples (Xing et al., 2014). Dendronan® demonstrated a mannose-to-glucose ratio of 6.9:1 and a weight average molecular weight (Mw) of 312 kDa. Methylation analysis indicated that Dendronan® was composed of →4)-Man*p*-(1→ and →4)-Glc*p*-(1→ and did not contain branches. 2D ^1H–^1H COSY and 2D ^1H–^1H TOCSY study indicated the substitution of acetyl groups at O-2 or O-3 position of some mannoses in Dendronan® (Xing et al., 2014). However, the relatively high viscosity of Dendronan® D_2O solution made it difficult to obtain high-resolution heteronuclear 2D ^1H–^{13}C NMR spectra such as 2D ^1H–^{13}C HMBC, 2D ^1H–^{13}C HMQC. Due to the lack of such heteronuclear 2D NMR spectra, only part of the signals from

* Corresponding author. Tel.: +1 226 217 8076; fax: +1 519 780 2600.
E-mail addresses: stevewcui@gmail.com, Steve.Cui@agr.gc.ca (S.W. Cui).

http://dx.doi.org/10.1016/j.carbpol.2014.08.121
0144-8617/

major residues of Dendronan® were assigned and more detailed structural information of the sample could not be obtained in the previous study (Xing et al., 2014).

An interesting finding from Xing et al. (2014) was that extensive mannanase hydrolysis of Dendronan® resulted in the production of *O*-acetyl group-rich oligosaccharides that were highly resistant to the enzymatic hydrolysis. This finding inspired us to hypothesize in the current study that the mannanase-resistant oligosaccharides, due to their low-molecular-weight and *O*-acetyl group-rich nature, could be dissolved in D_2O to form a solution with relatively low viscosity and high sample concentration, and such solution could provide full sets of high-resolution 2D NMR spectra with strong signals related to *O*-acetylated residues.

Recovering oligosaccharides from aqueous solutions using ethanol precipitation has been reported by some research groups (Ku, Jansen, Oles, Lazar, & Rader, 2003; Liu, Peng, & Liu, 2012; Price, Hartman, Faber, Vermillion, & Fahey, 2011; Roxas, Fukuba, & Mendoza, 1985; Sen et al., 2011; Swennen, Courtin, Van der Bruggen, Vandecasteele, & Delcour, 2005; Thurl, Offermanns, Müller-Werner, & Sawatzki, 1991; Xu, Lin, & Shi, 2011; Zhang, Zhang, & Wang, 2009). For example, using 50% (v/v) ethanol precipitation, Price et al. (2011) successfully recovered galactoglucomannan oligosaccharides from an acid-hydrolyzed molasses byproduct of pine fiberboard production. Although this method has the drawback of incomplete precipitation of oligosaccharides, it is simple and quick in obtaining relatively large amounts of sample (Ku et al., 2003). Therefore, in the current study, we attempted to use ethanol precipitation to collect oligosaccharides resulting from the hydrolysis of Dendronan® by mannanase, which was followed by obtaining a set of high-resolution 2D NMR spectra of the collected sample and extracting detailed structural information regarding the *O*-acetylated sugar residues and glycosidic linkages from the spectra obtained.

2. Materials and methods

2.1. Sample preparation

Dendronan® was extracted and purified as described in our previous report (Xing et al., 2014). The complete dissolution of Dendronan® (2 g) in 100 mL of de-ionized water in a 500 mL beaker was achieved by stirring and heating at 70 °C for 6 h, and then temperature of the solution was allowed to drop to 37 °C. Subsequently, 50 μL of endo-β-1,4-mannanase suspension (*Aspergillus niger*, Megazyme, Ireland,. 297 U/mL) was added to the solution, followed by stirring at 37 °C for 40 min. Immediately following the 40-min enzymatic treatment, the beaker was put in a 95 °C water bath with stirring for 20 min to deactivate the enzyme and then was allowed to cool at room temperature. Ethanol (31 mL) pre-cooled at 4 °C was added dropwise to the solution with vigorous stirring to form a mixture with an ethanol concentration of around 20% (w/w). After staying at 4 °C for 6 h, the mixture was centrifuged at 10,000 × *g* and 4 °C for 15 min. The minor amount of precipitate was discarded and the supernatant was transferred to a 500 mL beaker. Subsequently, 260 mL of 100% ethanol pre-cooled at −20 °C was added dropwise to the supernatant with vigorous stirring to form a suspension with an ethanol concentration of approximately 70% (w/w). The system was then kept at −20 °C for 12 h to facilitate the formation of precipitate, after which the precipitate was collected by centrifuge at 10,000 × *g* and 4 °C for 15 min. The collected precipitate was re-dissolved in de-ionized water (50 mL), and the resultant solution was frozen and freeze-dried to produce a dry sample (designated HDOP). HDOP was then subjected to Maldi-tof-MS analysis to obtain information about the distribution of molecular weight, according to Xing et al. (2014).

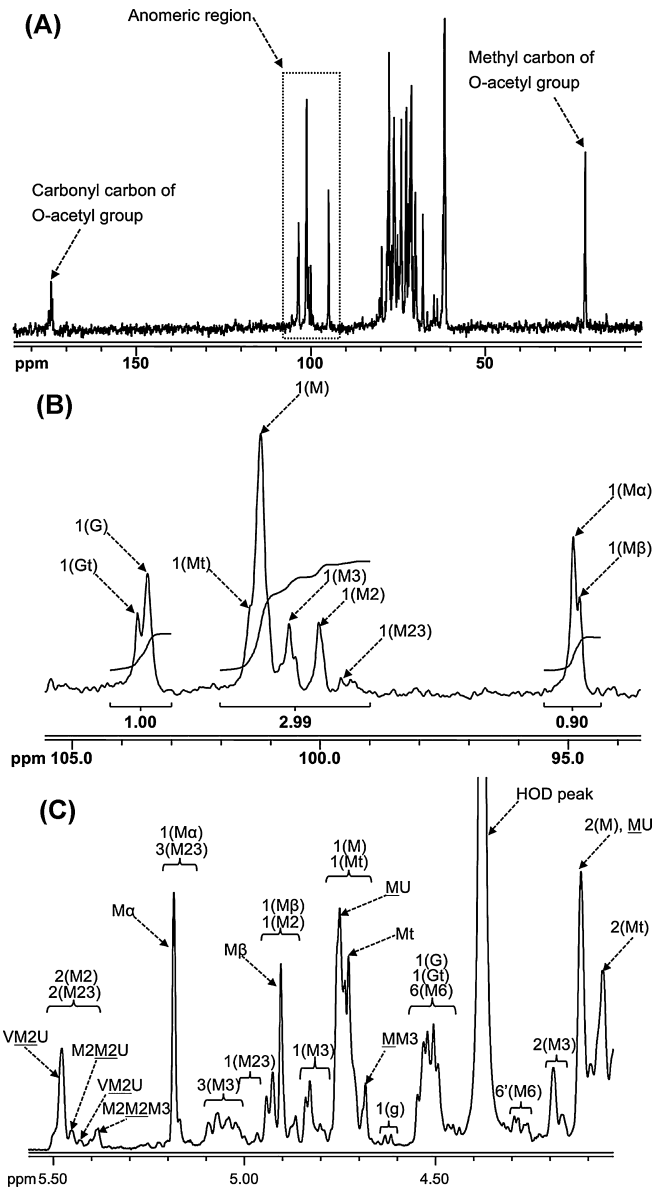

Fig. 1. 1D ^{13}C spectrum ((A) and (B)) and ^{1}H NMR spectrum (C) of HDOP. "U" means residues G, M, or M2 in the reducing end side. "V" means residue G, M, or M3 in the non-reducing end side. For example, 1(G) in figure (B) and figure (C) means the signal comes from the C-1 and H-1 of glucose residue G, respectively. 1(g) denotes the signal from H-1 of galactose residue (designated residue g) of β-(1 → 4)-D-galactan contaminant.

2.2. 1D and 2D NMR spectroscopy

The sample for 1D and 2D NMR spectroscopy was prepared by dissolving around 240 mg of HDOP in 5 mL of D_2O and then freeze-drying the solution; this dissolution-drying process was repeated three times. The sample recovered from the third freeze-drying treatment was re-dissolved in 4 mL of D_2O, passed through a nylon syringe filter (pore size 1.5 μm), and transferred to a regular NMR tube (5 mm). The ^{1}H and ^{13}C NMR spectra of the sample were acquired, respectively, at 500.13 and 125.78 MHz on a Bruker AMX 500FT NMR spectrometer (Bruker Co., Germany). A $^{1}H/^{13}C/^{15}N$ probe with 5-mm inverse geometry was used. Trimethylsilyl propionate (TSP) in D_2O and 1,4-dioxane in D_2O were used as ^{1}H and ^{13}C NMR chemical shift standards, respectively. 1D ^{1}H NMR experiment, 1D ^{13}C NMR experiment, and a series of 2D NMR experiments including 2D ^{1}H–^{1}H correlation NMR spectroscopy (COSY), 2D

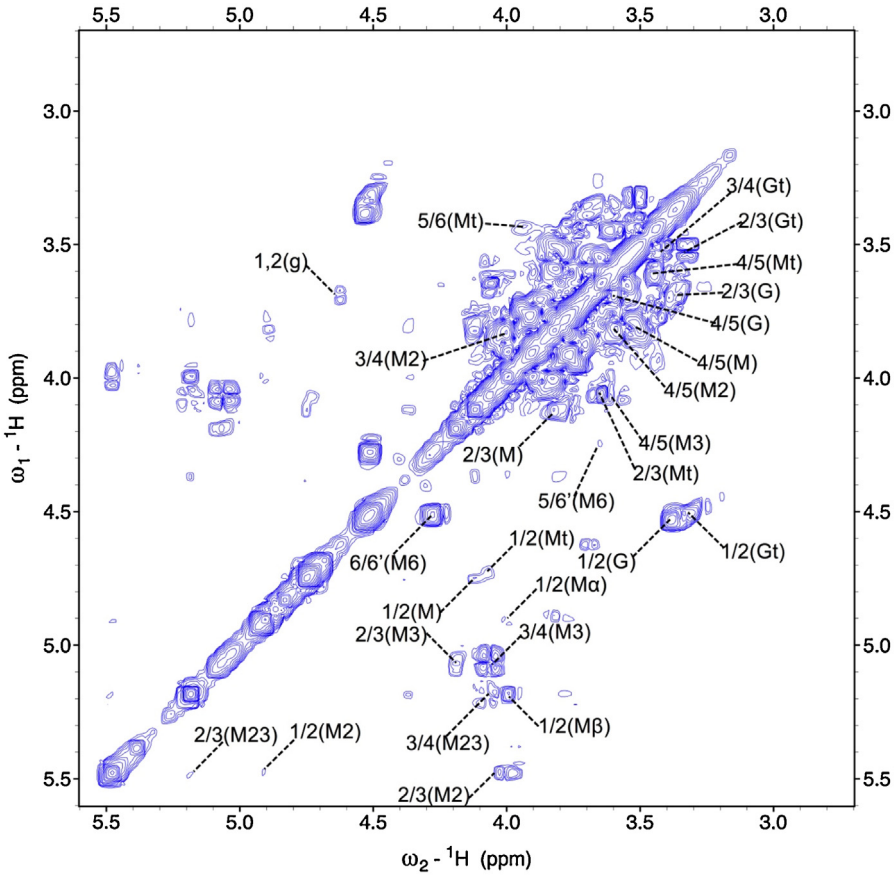

Fig. 2. COSY spectrum of HDOP. Correlations between neighboring proton atoms are marked. For example, "1/2(G)" means the cross-signal between H-1 and H-2 of the residue G.

^{1}H–^{1}H total correlation NMR spectroscopy (TOCSY), 2D ^{1}H–^{13}C heteronuclear multiple-bond NMR spectroscopy (HMBC), 2D ^{1}H–^{13}C heteronuclear multiple-quantum coherence NMR spectroscopy (HMQC), and 2D ^{1}H–^{1}H nuclear Overhauser effect spectroscopy (NOESY) were performed at 53 °C following the standard Bruker pulse sequences.

3. Results and discussion

MALDI-tof-MS analysis showed that HDOP was mainly composed of oligosaccharides with degrees of polymerization (DP) of 3–15 and was rich in *O*-acetyl groups. The yield of HDOP based on the dry weight of Dendronan® was only 24.7%, however, HDOP had much lower molecular weight and much more acetyl group substitution than Dendronan®, enabling the complete dissolution of HDOP in D_2O to form a clear solution (6%, w/w). And, as we expected, the sample solution generated strong signals in 1D ^{13}C spectrum (Fig. 1), 1D ^{1}H spectrum (Fig. 1), and a series of 2D NMR spectra including COSY (Fig. 2), TOCSY (Figs. 3 and 7), HMQC (Fig. 4), HMBC (Fig. 5), and NOESY (Fig. 8).

3.1. Evidence for the existence of O-acetyl groups

Two ^{13}C resonances at 174.2 ppm and 21.3 ppm in the 1D ^{13}C NMR spectrum (Fig. 1A) were assigned to carbonyl carbons and methyl carbons in *O*-acetyl groups, respectively, by referring to literature (Hannuksela & Hervé du Penhoat, 2004; van Hazendonk, Reinerik, de Waard, & van Dam, 1996). The assignment was supported by the 1D ^{1}H NMR signals at 2.11 ppm, 2.15 ppm, and 2.20 ppm from protons in *O*-acetyl groups and confirmed by the corresponding C/H correlations between methyl carbons and protons in *O*-acetyl groups in the HMQC spectrum and by the corresponding C/H cross-peak between carbonyl carbons and protons in *O*-acetyl groups in the HMBC spectrum.

3.2. Identification of residues without the substitution of O-acetyl groups

3.2.1. Residue G

The existence of →4)-β-D-Glc*p*-(1→ (designated residue G) was revealed by its characteristic H-1 and H-2 signals in the 1D ^{1}H NMR spectrum and its C-1 peak in the 1D ^{13}C NMR spectrum (Fig. 1), according to literature (Crescenzi et al., 2002; Hannuksela & Hervé du Penhoat, 2004; Katsuraya et al., 2003), and was further confirmed by cross-signals at 4.53 ppm/3.37 ppm (H-1/H-2) in the COSY spectrum (Fig. 2) and at 103.5 ppm/4.53 ppm (C-1/H-1) in the HMQC spectrum (Fig. 4). Once the chemical shift of H-2 was obtained, it was easy to find the cross-peak of H-2/H-3 (3.37 ppm/3.70 ppm) in the COSY spectrum (Fig. 2). Because the chemical shifts of H-3 and H-4 of residue G were very close to each other, the H-3/H-4 cross-peak of the residue was in the diagonal of the COSY spectrum (Fig. 2). A cross peak at 3.70 ppm/3.60 was assigned to H-4/H-5 correlation, with the H-5 chemical shift in good agreement with literature data (Crescenzi et al., 2002). The chemical shifts extracted from the COSY spectrum were verified by the cross-peaks of H-1/H-2 (4.53 ppm/3.37 ppm) as well as the overlapped cross-signals of H-1/H-3, H-1/H-4, and H-1/H-5 in the TOCSY spectrum (Fig. 3). The residue also generated cross-peaks at 3.37 ppm/74.1 ppm (H-2/C-2), 3.70 ppm/75.2 ppm (H-3/C-3), and 3.70 ppm/79.7 ppm (H-4/C-4) in the HMQC spectrum (Fig. 4). The

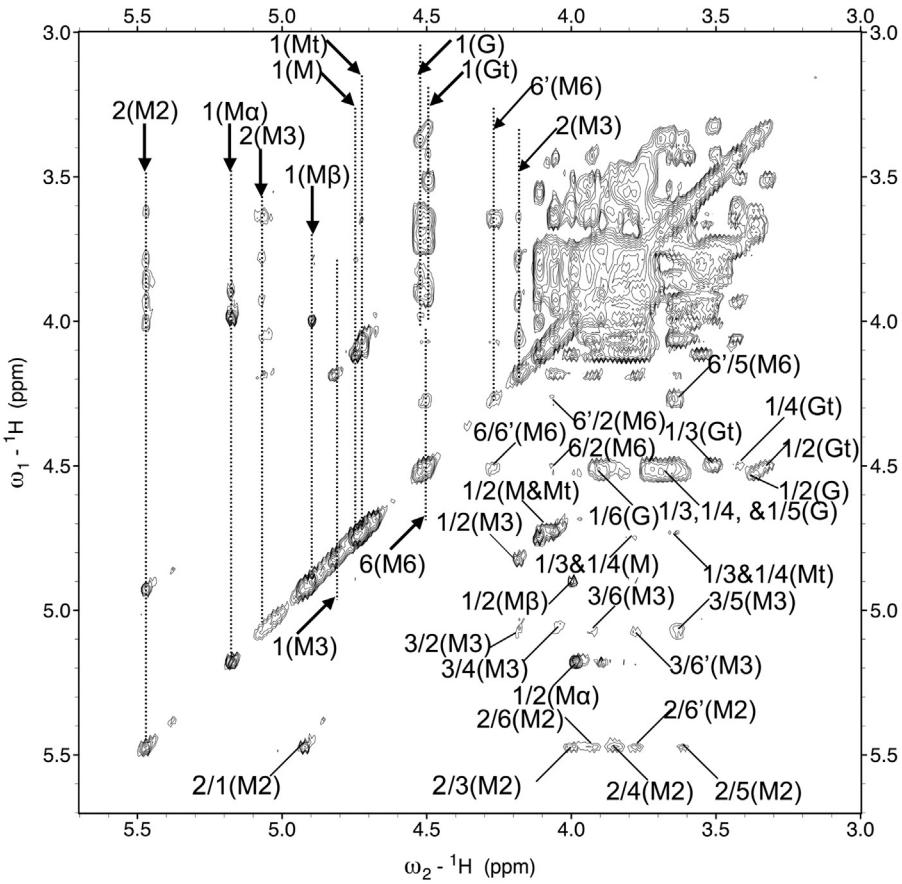

Fig. 3. TOCSY spectrum of HDOP. Both signal lines and cross-signals are marked. For example, "2(M2)" means signal line caused by H-2 of the residue M2. "2/3(M2)" means the cross-signal between H-2 and H-3 of the residue M2.

C-5/H-5 cross-peaks, despite overlapping with signals from other residues, demonstrated a C-5 chemical shift of 76.0 ppm. Both ^{1}H and ^{13}C chemical shifts of the residue were further confirmed by strong cross-peaks at 103.7 ppm/4.53 ppm (C-1/H-2), 75.2 ppm/3.69 ppm (C-3/H-2), 75.2 ppm/3.70 ppm (C-3/H-4), and 79.7 ppm/3.70 ppm (C-4/H-3) in the HMBC spectrum (Fig. 5). The chemical shift of C-6 was extracted from two cross-peaks at 61.5 ppm/3.60 ppm (C-6/H-5) and 61.5 ppm/3.70 ppm (C-6/H-4).

3.2.2. Residue Gt

It was found in literature that →4)-β-D-Glc*p*-(1→ residue and non-reducing end β-D-Glc*p*-(1→ residue differed greatly in H-3 and H-4 chemical shifts but were close to each other in the chemical shifts of other protons (Goldberg, Gillou, & Prat, 1991; Schröder et al., 2001; Tenkanen, Makkonen, Perttula, Viikari, & Teleman, 1997). In the current study, the existence of non-reducing end β-D-Glc*p*-(1→ (designated Gt) were indicated by the cross-peaks at 3.32 ppm/3.52 ppm (H-2/H-3) and 3.52 ppm/3.42 ppm (H-3/H-4) in the COSY spectrum (Fig. 2) and the cross-peaks at 4.51 ppm/3.52 ppm (H-1/H-3) and 4.51 ppm/3.42 ppm (H-1/H-4) in the TOCSY spectrum (Fig. 3). Once the chemical shifts of H-3 and H-4 of residue Gt were determined, the chemical shift of H-1 was easily obtained from the cross-peaks of H-1/H-2 (4.51/3.32) in the COSY spectrum (Fig. 2). Two cross-signals caused by C-3/H-3 and C-4/H-4 correlations of the residue were observed at 76.7 ppm/3.52 ppm and 70.7 ppm/3.42 ppm in the HMQC spectrum (Fig. 4), respectively. The C-1/H-1 (103.7 ppm/4.51 ppm) and C-2/H-2 (74.3 ppm/3.32 ppm) signals of residue Gt were overlapped with those of residue G in the HMQC spectrum (Fig. 4), because of the closeness of the two residues in the chemical shifts of C-1, H-1, C-2, and H-2. Signals at 70.7 ppm/3.52 ppm (C-4/H-3), 76.7 ppm/3.42 ppm (C-3/H-4), and 70.7 ppm/3.32 ppm (C-4/H-2) in the HMBC spectrum (Fig. 5) further verified the chemical shifts of C-4, H-4, C-3, H-3, and H-2.

3.2.3. Residue M

The presence of →4)-β-D-Man*p*-(1→ (designated residue M) was indicated by sharp peaks at around 101.3 ppm and 4.75 ppm in the ^{13}C NMR spectrum (Fig. 1B) and the ^{1}H NMR spectrum, respectively (Fig. 1C), according to literature (Crescenzi et al., 2002; van Hazendonk et al., 1996). Knowing the ^{1}H chemical shift of H-1 enabled us to sequentially assign the cross-peaks of H-1/H-2 (4.75 ppm/4.12 ppm), H-2/H-3 (4.12 ppm/3.82 ppm), H-4/H-5 (3.78 ppm/3.56 ppm), and H-5/H-6 (3.51 ppm/3.94 ppm) in the COSY spectrum (Fig. 2). Cross-peak of H-3/H-4 of the residue was too close to the diagonal to be observable in the COSY spectrum (Fig. 2), very similar to the case in residue G. Compared with other major residues in HDOP, residue M demonstrated much less signals in the TOCSY spectrum (Fig. 3). There were only H-1/H-2 (4.75 ppm/4.12 ppm), H-1/H-3 (4.75 ppm/3.82 ppm), and H-1/H-4 (4.75 ppm/3.78 ppm) cross-peaks observed in Fig. 3, despite the relatively high concentration of the NMR sample in the current study. Based upon the ^{1}H chemical shifts obtained, the C-1/H-1 (101.2 ppm/4.75 ppm), C-2/H-2 (71.1 ppm/4.12 ppm), and C-3/H-3 (72.6 ppm/3.82 ppm) cross-peaks of residue M were easily found in the HMQC spectrum (Fig. 4). C-5/H-5 and C-4/H-4 cross-peaks of the residue were found overlapped with signals from other residues in the HMQC spectrum (Fig. 4), but such overlapping did

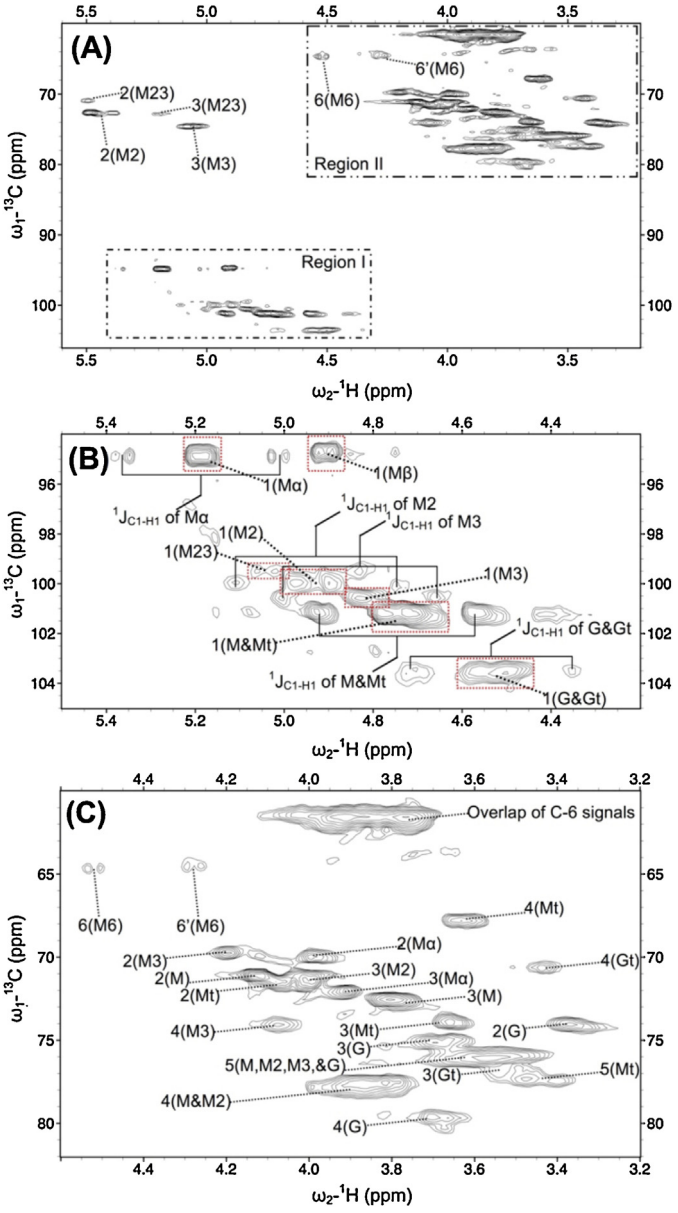

Fig. 4. HMQC spectrum of HDOP. The squared regions I and II in figure (A) are enlarged and shown as figure (B) and figure (C), respectively. For example, "1(M2)" means the C-1/H-1 cross-point of the residue M2. The bracketed signals demonstrate C–H coupling.

not affect the extraction of ^{13}C chemical shifts of C-4 and C-5. In the HMBC spectrum (Fig. 5), the C-1/H-2 (101.2 ppm/4.12 ppm), C-3/H-1 (72.6 ppm/4.75 ppm), C-4/H-2 (77.5 ppm/4.12 ppm), C-4/H-3 (77.5 ppm/3.82 ppm), and C-5/H-3 (76.0 ppm/3.82 ppm) cross-peaks were identified, verifying the ^{1}H and ^{13}C chemical shifts obtained. Besides, the C-3/H-4 (72.6 ppm/3.78 ppm) and C-5/H-4 (76.0 ppm/3.78 ppm) correlation signals of residue M were overlapped with those produced by other residues.

3.2.4. Residue Mt

Compared with Dendronan®, HDOP gave rise to four new peaks at 4.72 ppm/4.07 ppm, 3.62 ppm/3.44 ppm, 3.44 ppm/3.78 ppm, and 3.44 ppm/3.94 ppm in the COSY spectrum (Fig. 2), which were respectively assigned to the H-1/H-2, H-4/H-5, H-5/H-6′, and H-5/H-6 correlations of non-reducing end β-D-Man*p*-(1→ (designated residue Mt), according to literature (Goldberg et al., 1991; Hannuksela & Hervé du Penhoat, 2004; Tenkanen et al., 1997). The H-3/H-4 cross-peak (3.66 ppm/3.62 ppm) was too close to the diagonal to be observed in the COSY spectrum (Fig. 2). In the TOCSY spectrum (Fig. 3), the H-1/H-2 cross-signal of residue Mt was overlapped with that of residue M, however, the H-1/H-3 (4.72 ppm/3.66 ppm) and H-1/H-4 (4.72 ppm/3.62 ppm) cross-peaks of the former residue were quite differentiable with those of the latter one. In the HMQC spectrum (Fig. 4), the C-1/H-1 signal (101.4 ppm/4.72 ppm) of residue Mt was overlapped with that of residue M. The cross-peaks at 71.5 ppm/4.07 ppm, 73.9 ppm/3.66 ppm, 67.8 ppm/3.62 ppm, and 77.4 ppm/3.44 ppm were assigned to the C-2/H-2, C-3/H-3, C-4/H-4, and C-5/H-5 correlations of residue Mt, respectively. These ^{1}H and ^{13}C chemical shifts was further confirmed by the signals at 101.4 ppm/4.07 ppm (C-1/H-2), 73.9 ppm/4.72 ppm (C-3/H-1), 67.8 ppm/4.07 ppm (C-4/H-2), 67.8 ppm/3.66 ppm (C-4/H-3), 73.9 ppm/3.62 ppm (C-3/H-4), 73.9 ppm/4.07 ppm (C-3/H-2), and 77.4 ppm/3.66 ppm (C-5/H-3) in the HMBC spectrum (Fig. 5).

3.2.5. Residue Mα

The cross-peak at 5.18 ppm/3.99 ppm in the COSY spectrum (Fig. 2) was assigned to the H-1/H-2 correlation of reducing end →4)-α-D-Man*p* residue (designated residue Mα), according to literature (Goldberg et al., 1991; Hannuksela & Hervé du Penhoat, 2004; Lundqvist et al., 2002; Tenkanen et al., 1997). This assignment was supported by the H-1/H-2 correlation at 5.18 ppm/3.99 ppm in the TOCSY spectrum (Fig. 3). In the HMQC spectrum (Fig. 4), the C-1/H-1 (94.9 ppm/5.18 ppm), C-2/H-2 (70.1 ppm/3.99 ppm), and C-3/H-3 (72.0 ppm/3.91 ppm) correlations were found. The chemicals shifts of H-1, H-2, H-3, C-1, C-2, and C-3 of Mα were further confirmed by the C-2/H-1 (70.1 ppm/5.18 ppm), C-3/H-1 (72.0 ppm/5.18 ppm), and C-3/H-2 (72.0 ppm/3.99 ppm) cross-peaks in the HMBC spectrum (Fig. 5).

3.2.6. Residue Mβ

The signal at 4.91 ppm/4.00 ppm in either the COSY (Fig. 2) and the TOCSY spectrum (Fig. 3) was caused by the H-1/H-2 correlation of reducing end →4)-β-D-Man*p* residue (designated Mβ), with reference to literature (Goldberg et al., 1991; Hannuksela & Hervé du Penhoat, 2004; Lundqvist et al., 2002; Tenkanen et al., 1997). ^{13}C chemical shift of the C-1 of residue Mβ was obtained from the C-1/H-1 cross-peak at 4.91 ppm/94.8 ppm in the HMQC spectrum (Fig. 4). According to the reported ^{13}C chemical shift of the C-2 of residue Mβ (Goldberg et al., 1991; Hannuksela & Hervé du Penhoat, 2004), the cross-peak at 71.9 ppm/4.91 ppm in the HMBC spectrum was assigned to the C-2/H-1 correlation of the residue.

3.3. Identification of residues with the substitution of O-acetyl groups

3.3.1. Residue M2

The strong ^{1}H resonance at 5.47 ppm (Fig. 1) was assigned to H-2 of →4)-2-*O*-acetyl-β-D-Man*p*-(1→ (designated residue M2), according to literature data (Hannuksela & Hervé du Penhoat, 2004; Lundqvist et al., 2002; Teleman, Nordström, Tenkanen, Jacobs, & Dahlman, 2003; van Hazendonk et al., 1996). The cross-peaks between the H-2 (5.47 ppm) of M2 and each of H-1 (4.92 ppm), H-3 (4.00 ppm), H-4 (3.85 ppm), H-5(3.61 ppm), H-6′ (3.78 ppm), and H-6 (3.93 ppm) in the residue were found in the TOCSY spectrum (Fig. 3). The assignment was proved to be correct by the corresponding cross-signals of H-1/H-2 (4.92 ppm/5.47 ppm), H-2/H-3 (5.47 ppm/4.00 ppm), H-3/H-4 (4.00 ppm/3.85 ppm), H-4/H-5 (3.85 ppm/3.61 ppm), and H-5/H-6′ (3.61 ppm/3.78 ppm) in the COSY spectrum (Fig. 2). Some ^{13}C chemical shifts of residue M2 were extracted from the cross-peaks of C-1/H-1 (100.0 ppm/4.92 ppm), C-2/H-2 (72.6 ppm/5.47 ppm), C-3/H-3

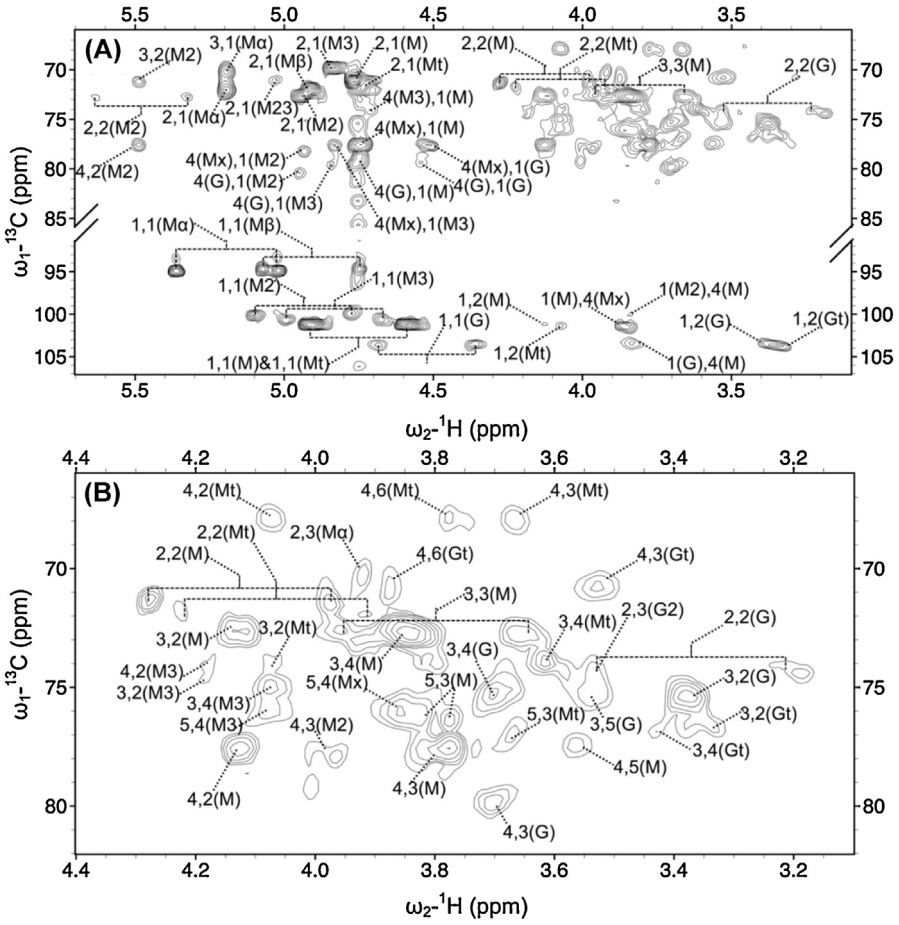

Fig. 5. HMBC spectrum of HDOP. Both inter- and intra-residual correlation are marked in figure (A). figure (B) shows the detailed peak assignment in the region with ^{1}H and ^{13}C chemical shift ranges of 3.0–4.4 ppm and 66–82 ppm, respectively. For example, "3,2(M2)" means the cross-peak between the C-3 and H-2 of the residue M2. "4(G), 1(M)" means the cross-signal between C-4 of the residue G and H-1 of the residue M. "Mx" means "M2" or "M". The bracketed signals demonstrate C–H coupling.

(71.4 ppm/4.00 ppm), C-4/H-4 (77.6 ppm/3.85 ppm), and C-5/H-5 (76.0 ppm/3.61 ppm) in the HMQC spectrum (Fig. 4) and were further confirmed by the C-2/H-1 (72.6 ppm/4.92 ppm), C-4/H-2 (77.6 ppm/5.47 ppm), C-3/H-2 (71.4 ppm/5.47 ppm), and C-4/H-3 (77.6 ppm/4.00 ppm) in the HMBC spectrum (Fig. 5). The correlation between carbonyl carbon of *O*-acetyl groups and H-2 of M2 was found at 174.2 ppm/5.47 ppm in HMBC.

3.3.2. Residue M3

The existence of →4)-3-*O*-acetyl-β-D-Man*p*-(1→ (designated residue M3) was indicated by its characteristic H-3 signal at 5.07 ppm (Fig. 1), according to literature (Hannuksela & Hervé du Penhoat, 2004; Lundqvist et al., 2002; Teleman et al., 2003; van Hazendonk et al., 1996). The presence of M3 was verified by strong cross-signals of H-3/H-1 (5.07 ppm/4.83 ppm), H-3/H-2 (5.07 ppm/4.18 ppm), H-3/H-4 (5.07 ppm/4.04 ppm), H-3/H-5 (5.07 ppm/3.63 ppm), H-3/H-6′ (5.07 ppm/3.78 ppm), and H-3/H-6 (5.07 ppm/3.93 ppm) in the TOCSY spectrum (Fig. 3) and by cross-peaks of H-1/H-2 (4.83 ppm/4.18 ppm), H-2/H-3 (4.18 ppm/5.07 ppm), H-3/H-4 (5.07 ppm/4.04 ppm), and H-4/H-5 (4.04 ppm/3.63 ppm) in the COSY spectrum (Fig. 2). The correlation between H-1 and H-2 (4.83 ppm/4.18 ppm) was also observable in the TOCSY spectrum (Fig. 3). In the HMQC spectrum (Fig. 4), the ^{1}H signals at 4.83 ppm (H-1), 4.18 ppm (H-2), 5.07 ppm (H-3), 4.04 ppm (H-4), and 3.63 ppm (H-5) of M3 were correlated with the ^{13}C signals at 100.6 ppm (C-1), 69.8 ppm (C-2), 74.6 ppm (C-3), 74.1 ppm (C-4), and 75.8 ppm (C-5), respectively. These correlations were supported by cross-signals at 69.8 ppm/4.83 ppm (C-2/H-1), 74.6 ppm/4.18 ppm (C-3/H-2), 74.1 ppm/4.18 ppm (C-4/H-2), and 74.6 ppm/4.04 ppm (C-3/H-4) in the HMBC spectrum (Fig. 5). Carbonyl carbon of *O*-acetyl groups was found correlated with the H-3 of M3 at 174.1 ppm/5.08 ppm in HMBC.

3.3.3. Residue M23

Because ^{1}H chemical shifts were more sensitive to the attachment of electronegative *O*-acetyl groups than ^{13}C chemical shifts, the cross-peak between acetylated C-2 (C-3) and corresponding H-2 (H-3) was always found in the less crowded upper left area in HMQC spectra like Fig. 4A in the current study or HSQC spectra in previous studies (Rakhimov, Shashkov, Zhauynbaeva, Malikova, & Abdullaev, 2004; van Hazendonk et al., 1996). Besides, the cross-peaks of acetylated C-2/H-2 and acetylated C-3/H-3 of →4)-2,3,6-tri-*O*-acetyl-β-D-Manp-(1→ residues (designated M236) were both found in the upper left region of HMBC spectra (Jakes, Yelle, & Frihart, 2011). The very downfield chemical shifts of H-2 and H-3 in M236 apparently resulted from the substitution of *O*-acetyl groups at both O-2 and O-3 position. Furthermore, it was reasonable to deduce that →4)-2,3-di-*O*-β-D-Man*p*-(1→ residues (designated M23) could give rise to C-2/H-2 and C-3/H-3 cross-peaks at the same region of HMQC spectra as M236 did, because of the finding that the absence or presence of an acetyl group at the O-6 position had little effects on the chemical shifts of H-2, H-3, C-2, and C-3 of a 1 → 4 linked β-D-Man*p* residue (Rakhimov et al., 2004). In the current study, aside from C-2/H-2 signal of M2 and C-3/H-3

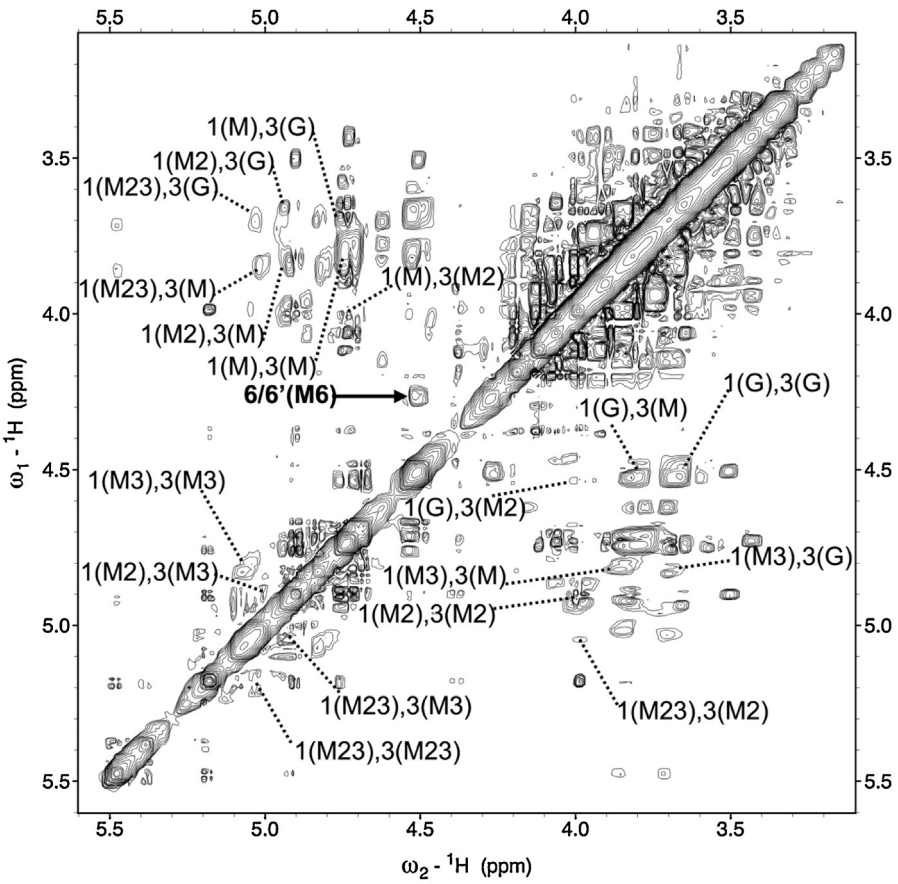

Fig. 6. NOESY spectrum of HDOP. Cross-signals are marked. For example, "1(G), 3(M)" means correlation between H-1 of the residue G and H-3 of the residue M.

signal of the M3, there were two more cross-peaks in the upper left region of Fig. 4A. The two unassigned peaks at 70.9 ppm/5.49 ppm and 72.8 ppm/5.21 ppm were assigned as the C-2/H-2 and C-3/H-3 correlations of M23, respectively. The assignment was then supported by the cross-signal at 5.49 ppm/5.21 ppm (H-2/H-3) in both the COSY spectrum (Fig. 2) and the TOCSY spectrum with a small minimum contour level (Fig. 7). The cross-signal at 5.21 ppm/4.07 ppm in the COSY spectrum (Fig. 2) was assigned to the H-3/H-4 correlation of M23, and this assignment was confirmed by the cross-peak at 5.21 ppm/4.07 ppm (H-3/H-4) in the TOCSY spectrum (Fig. 7). The signal at 5.49 ppm/5.02 ppm in the TOCSY was assigned to the H-2/H-1 correlation of M23. The correctness of the H-1 chemical shift was confirmed by the signal at 71.2 ppm/5.02 ppm (C-2/H-1) in HMBC (Fig. 5). The observation of a weak signal at 99.5 ppm/5.02 ppm in the anomeric region of the spectrum was apparently caused by the C-1/H-1 correlation of M23. Though the correlation between the carbonyl carbon of *O*-acetyl group and the H-2 or H-3 of the residue was not detectable in the HMBC spectrum (Fig. 5), this did not disprove the existence of M23, given the fact that the amount of M23 was very low in the sample.

We found that the H-1 chemical shift of mannose residues decreased following the order of M23, M2, M3, and M. This is reasonable. Since *O*-acetyl groups are more electronegative than hydroxyl groups, two *O*-acetyl groups at both C-2 and C-3 have larger de-shielding effect on H-1 compared with single *O*-acetyl group at either C-2 or C-3. *O*-acetyl group is closer to H-1 in M2 than in M3, resulting in the H-1 in the former residue being more de-shielded than that in the latter one.

There were considerable differences in C-4 chemical shift between M and M3, in C-3 chemical shift between M and M2 and between M3 and M23, in C-2 chemical shift between M and M3 and between M2 and M23, and in C-1 chemical shift between M and M2, observed in the current study. This finding indicated that the attachment of an *O*-acetyl group to a carbon of 1 → 4 linked β-D-Man*p* ring could shield the nuclei of adjacent carbons in the same ring.

3.3.4. *Residue M6, residue M26, and residue M36*

In the TOCSY spectrum with a relatively small minimum contour level (Fig. 7), we found evidences for the existence of →4)-6-*O*-acetyl-β-D-Man*p*-(1→ (designated residue M6), →4)-2,6-di-*O*-acetyl-β-D-Man*p*-(1→ (designated residue M26), and →4)-3,6-di-*O*-acetyl-β-D-Man*p*-(1→ (designated M36). Assignments were according to literature data (Rakhimov et al., 2004). The existence of M6 was supported by its strong H-6′/H-6 (4.28 ppm/4.51 ppm) correlation in both COSY (Fig. 2) and TOCSY (Figs. 3 and 7) spectra, and was further confirmed by C-6/H-6 (64.6 ppm/4.51 ppm) and C-6/H-6′ (64.6 ppm/4.28) cross-peaks in the HMQC spectrum (Fig. 4). Two cross signals at 3.65 ppm/4.28 ppm and 3.65 ppm/4.51 ppm observed in both COSY and TOCSY spectra were assigned to H-5/H-6′ and H-5/H-6 of M6, respectively. Besides, the correlations of H-6/H-2 (4.51 ppm/4.13 ppm) and H-6′/H-2 (4.28 ppm/4.13) were found in the TOCSY spectrum (Figs. 3 and 7). Weak H-1/H-6 (4.74 ppm/4.51 ppm) and H-1/H-6′ (4.74 ppm/4.28 ppm) cross-signals were found in the TOCSY spectrum with small minimum contour level (Fig. 7). The chemical shifts of H-1, H-2, H-6, and H-6′ obtained in the current study were consistent with literature data

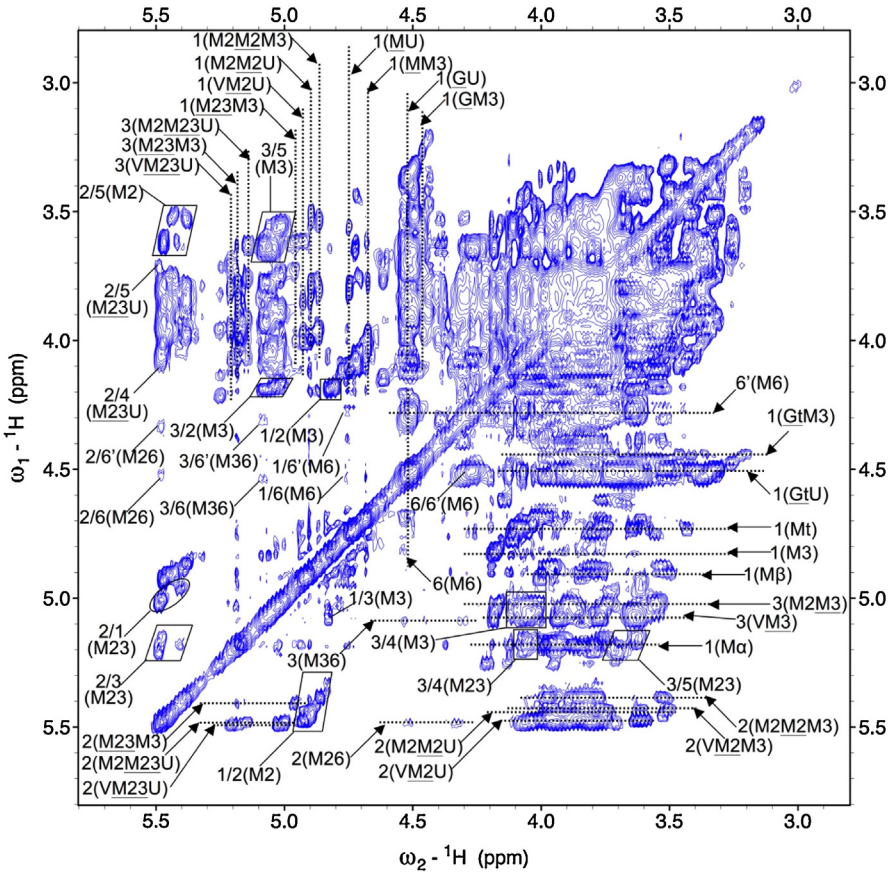

Fig. 7. TOCSY spectrum of HDOP, with low contour level. For example, "2(M2)" means the signal line is caused by H-2 of the residue M2. "2/3(M2)" means the cross-signal between H-2 and H-3 of the residue M2. "U" means residues G, M, or M2 in the reducing end side. "V" means residue G, M, or M3 in the non-reducing end side.

(Rakhimov et al., 2004). The H-5 chemical shift was a little smaller than the reported value, probably due to the effects of neighbouring residues with acetyl groups. The existence of M26 was supported by H-2/H-6 (5.48 ppm/4.52 ppm) and H-2/H-6′ (5.48 ppm/4.33 ppm) cross-peaks. The presence of M36 was indicated by H-3/H-6 (5.09 ppm/4.53 ppm) and H-3/H-6′ (5.09 ppm/4.31 ppm) cross-signals. The H-6/H-6′ cross-signals of M26 and M36 residues were overlapped with those of M6 residues, indicating that the effects of acetyl group substation at O-2 or O-3 position had very small effects on the chemical shifts of H-6 of 1 → 4 linked mannoses.

3.4. Glycosidic linkages between sugar residues

In the HMBC spectrum (Fig. 5), it was easy to find inter-residual cross-peaks of C-4 of G/H-1 of M2, C-4 of G/H-1 of M3, C-4 of G/H-1 of M, and C-4 of G/H-1 of G. Because the C-4 chemical shifts of M and M2 were close to each other, the cross-signals of C-4 of M2/H-1 of M2, C-4 of M2/H-1 of M3, C-4 of M2/H-1 of M, and C-4 of M2/H-1 of G overlapped with those between C-4 of M and H-1 of each M2, M3, M, and G. Although not observable in Fig. 5, cross-peaks of C-4 of M3/H-1 of M2, C-4 of M3/H-1 of M3, C-4 of M3/H-1 of M, and C-4 of M3/H-1 of G were observed when a lower minimum contour level was applied. The results indicated that, in a 1 → 4 linked β-D-glucomannan, the attachment of M3 to the O-1 position of a residue had larger shielding effect on the H-1 of the residue than the substitution of G, M, or M2 to the same position. It was also apparent that the attachment of M2 to the O-4 position of a residue resulted in a more de-shielded C-4 of the residue compared with the attachment of G, M, or M3 to the same position. Compared with these inter-residual C-4/H-1 correlations, inter-residual C-1/H-4 cross-signals of HDOP were much weaker in the HMBC spectrum (Fig. 5). We found correlations between C-1 of M2 and H-4 of M2, between C-1 of G and H-4 of M2, and between C-1 of G and H-4 of M. The cross-peaks of C-1 of M/H-4 of M2 and C-1 of Mt/H-4 of M2 were overlapped, resulting in a very strong signal in the HMBC spectrum (Fig. 5).

Because NOESY experiment shares part of its pulse sequences with COSY experiment, NOESY spectrum contains not only NOE signals but also COSY-like signals (Bubb, 2003; Reynolds & Enríquez, 2002). In the current study, COSY-like signals in the NOESY spectrum (Fig. 6) matched with those in the COSY spectrum. Furthermore, NOE signals in the NOESY spectrum (Fig. 6) provided much information about glycosidic linkages of HDOP. Consistent with previous NMR studies of 2,3-*O*-β-D-glucomannan (Hannuksela & Hervé du Penhoat, 2004; Hsieh et al., 2008), we found that NOE signals were generated between H-1 of a residue and H-3 of its neighboring residue on the reducing end side (Fig. 6). We noticed that H-3 of M3 correlated with H-1 of M-2 at 5.02 ppm/4.86 ppm, confirming the existence of diad M2M3. Apparently, the H-3 of M3 in the diad M2M3 was more upfield than the major H-3 signal (5.08 ppm) shown in the TOCSY spectrum with a high minimum contour level (Fig. 2). We then applied a relatively low minimum contour level to demonstrate the TOCSY data and found two sets of H-3 signals of M3 residues in the resultant spectrum (Fig. 6), with the upfield H-3 signal exactly the same as the aforementioned H-3 signal (5.02 ppm) in the NOESY spectrum (Fig. 6). Two research groups reported a considerably smaller H-3 chemical shift of M3 in M2M3 than in MM3, GM3, or M3M3,

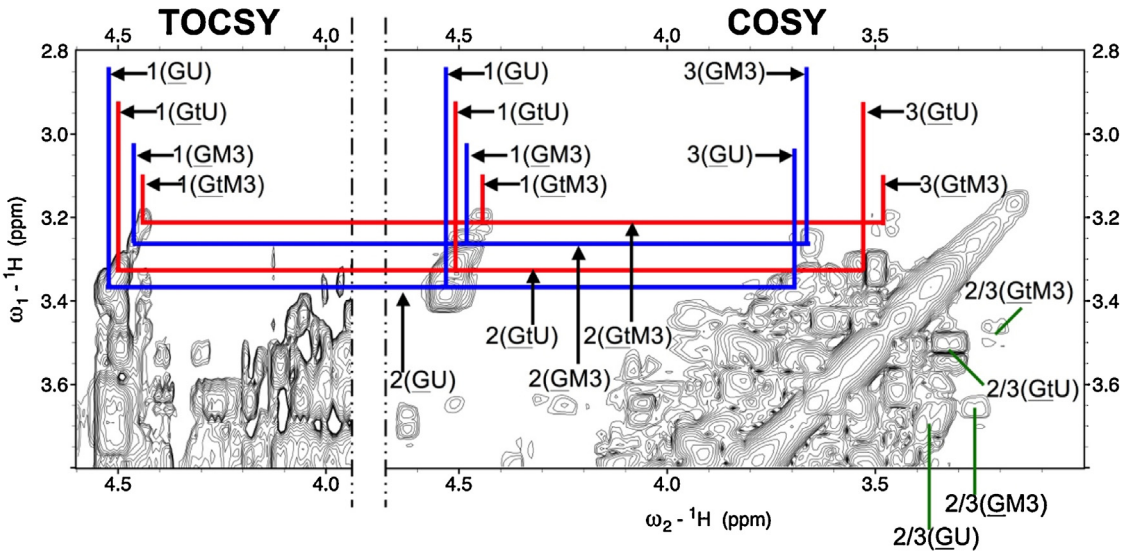

Fig. 8. A combined spectrum of TOCSY and COSY showing the multiple signal sets of the residue G and the residue Gt. "U" means residue G, M, or M2 in the reducing end side.

and the H-3 signals of M3 in MM3, GM3, and M3M3 were close to each other in either report (Hannuksela & Hervé du Penhoat, 2004; van Hazendonk et al., 1996). In view of this, we assigned the two signals at 5.02 ppm and 5.08 ppm to the H-3 of M3 in M2M3 and VM3, respectively, with V representing G, M, or M3. Furthermore, we found the M3 in M2M3 demonstrated considerably lower H-5, H-6, and H-6′ chemical shifts than the M3 in VM3, while there were no variations in the H-4 signals of M3 between them. These results indicated that M2 was capable of significantly shielding the H-3, H-5, H-6, and H-6′ of its neighboring residue on reducing end side. We named this phenomenon "M2 effect". Besides, the effect was also supported by the observation that H-3 of G had correlation with H-1 of M2, H-1 of M, and H-1 of M3 at 3.66 ppm/4.93 ppm, 3.70 ppm/4.75 ppm, and 3.70 ppm/4.83 ppm, respectively, in the NOESY spectrum (Fig. 6), indicating that a residue G with O-4 attachment to M2 had lower H-3 chemical shift than that with O-4 substitution of M or M3.

Besides, we found in the NOESY spectrum (Fig. 6) that H-1 of M23 formed cross-peaks with H-3 of M3, H-3 of M2, H-3 of M, and H-3 of G at 4.96 ppm/5.03 ppm, 5.04 ppm/3.97 ppm, 5.02 ppm/3.83 ppm, and 5.03 ppm/3.70 ppm, respectively. These results confirmed the aforementioned principle deduced from HMBC that a M3 residue had higher shielding effect on H-1 of its neighboring residue on non-reducing end side compared with M, G, or M2. We named this effect as "M3 effect". This effect was also supported by the reported chemical shift data of 2,3-*O*-acetyl glucomannan (Hannuksela & Hervé du Penhoat, 2004; van Hazendonk et al., 1996). In the current study, M23 demonstrated an H-1/H-2 signal of 4.96 ppm/5.41 ppm in the TOCSY spectrum (Fig. 7), which was related to the H-1 of M23/H-3 of M2 (4.96/5.03) cross-peak in the NOESY spectrum (H-6). Thus, we assigned the signal line at 5.41 ppm to H-2 of M23 in M23M3 and the signal lines at 5.48 ppm and 5.49 ppm to H-2 of M23 in M23U, with U being M2, M, or G. H-3 signals at 5.15 ppm and 5.21 ppm were correlated with the H-2 signals at 5.49 ppm and 5.48 ppm, respectively. The H-1 signal line (4.96 ppm) and the H-3 signal line (5.18 ppm) of M23 in M23U were close to the H-1 signal line of Mβ and the H-1 signal line of Mα, respectively. Considering the aforementioned "M2 effect", the two signals at 5.49 ppm and 5.48 ppm were further assigned to H-2 of M23 in the triads of VM23U and M2M23U, respectively. The H-2/H-5 and H-3/H-5 cross-peaks of M23 in VM23U were found respectively in the H-2 and H-3 signal lines of the residue in the TOCSY spectrum (Fig. 7). The H-3/H-5 cross-peak of M23 in M2M23U appeared at 5.15 ppm/3.63 ppm in the H-3 signal line of the residue, and its H-2/H-5 cross-signal was overlapped with that of M2. The "M2 effect" was also supported by the observation that H-1 of M2 correlated with H-3 of M3, H-3 of M, and H-3 of G at 4.86 ppm/5.02 ppm, 4.92 ppm/3.82 ppm, and 4.93 ppm/3.66 ppm in the NOESY spectrum (Fig. 6). H-2/H-1 cross-peaks at 5.47 ppm/4.93 ppm and 5.38 ppm/4.86 ppm were observed in the TOCSY spectrum with relatively low minimum contour level (Fig. 7), confirming the existence of M2M3 and M2U, respectively. Furthermore, M2 in M2M3 had a H-2/H-3 cross-peak at 5.47 ppm/4.00 ppm (Fig. 6), with the H-3 (4.00 ppm) forming NOE signals with H-1 of M (4.75 ppm) and H-1 of G (4.53 ppm) (Fig. 6). This indicated the H-2 signal line (5.47 ppm) was resulted from the M2 in triad VM2U, and this assignment was supported by the relatively upfield H-5 chemical shift (3.61 ppm) of the M2 (Fig. 7). According to the "M2 effect", the signal line at 5.38 ppm was further assigned to the H-2 of M2 in triad M2M2M3, noticing the relatively upfield H-3 at 3.96 ppm and H-5 signals at 3.53 ppm. Based on the chemical shifts of H-1, H-2, H-3, and H-5, two weak signal lines at 5.44 ppm and 5.42 were assigned to the H-2 in M2M2U and VM2M3, respectively, with the former assignment in agreement with the previous report that the signal at around 5.45 ppm was attributed to the H-2 of M2 in M2M2 (van Hazendonk et al., 1996). Multiple H-1 signal lines of M2 were found around the single H-1 signal line of Mα in the TOCSY spectrum (Fig. 6).

We further applied the "M2 effect" and "M3 effect" to assign signal sets of other residues. Gt demonstrated two signals sets in the TOCSY spectrum (Fig. 6). The chemical shift differences of H-2, H-1, and H-3 between the two signal sets made it reasonable to assign them to GtU and GtM3, according to "M3" effect. Similarly, two signal sets of G with chemical shifts different in H-2, H-3, and H-1 were assigned to GU and GM3. The signal features of G and Gt were also reflected in a combined figure of COSY and TOCSY (Fig. 8). We found single Mt signals and double M and M6 signal sets in the TOCSY spectrum (Fig. 6). Also, the "M3 effect" allowed us to assign the multiple signal sets of M and M6, based on the multiple H-1 and H-2 signals of these residues. For example, two sets of H-6/H-2, H-6′/H-2, and H-1/H-2 signals of M6 were found in

Table 1
^{1}H and ^{13}C of sugar residues in HDOP.

Residues	Signal intensity		1	2	3	4	5	6′	6	Linkages
M	Strong	δ_H	4.75	4.12	3.82	3.78	3.56	–	–	MU
		δ_C	101.2	71.1	72.6	77.5	76.0	61.7		
	Weak	δ_H	4.68	4.04	3.78	3.78	3.52	–	–	MM3
Mt	Strong	δ_H	4.72	4.07	3.66	3.62	3.44	3.78	3.94	MtU
		δ_C	101.4	71.5	73.9	67.8	77.4	61.7		
	Weak	δ_H	4.68	3.99	3.62	–	–	–	–	MtM3
Mα	Strong	δ_H	5.18	3.99	3.91	–	–	–	–	–
		δ_C	94.9	70.1	72.0	–	–	–	–	
Mβ	Strong	δ_H	4.91	4.00	–	–	–	–	–	–
		δ_C	94.8	71.9	–	–	–	–	–	
M2	Strong	δ_H	4.93	5.47	4.00	3.85	3.61	3.78	3.93	VM2U
		δ_C	100.0	72.6	71.4	77.6	76.0	61.7		
	Weak	δ_H	4.90	5.44	–	3.85	3.53	3.75	–	M2M2U
		δ_C	–	72.8	–	–	–	61.7		
	Weak	δ_H	4.88	5.42	–	–	3.61	–	–	VM2M3
		δ_C	–	72.7	–	–	–	61.7		
	Weak	δ_H	4.86	5.38	3.96	3.85	3.53	3.75	–	M2M2M3
		δ_C	–	72.7	–	–	–	61.7		
M3	Strong	δ_H	4.83	4.18	5.08	4.04	3.63	3.78	3.93	VM3
		δ_C	100.6	69.8	74.6	74.1	75.8	61.7		
	Weak	δ_H	4.80, 4.83	4.16	5.02	4.04	3.56	3.74	3.88	M2M3
M23	Weak	δ_H	5.02	5.49	5.21	4.07	3.72	3.80	3.95	VM23U
		δ_C	99.5	70.9	72.8	–	–	–		
	Weak	δ_H	5.00	5.48	5.15	4.07	3.63	3.75	–	M2M23U
	Weak	δ_H	4.96	5.41	5.18	4.07	–	–	–	M23M3
		δ_C	–	70.9	–	–	–	–		
M6	Weak	δ_H	4.69	4.07	–	–	3.65	4.31	4.53	M6M3
		δ_C	–	–	–	–	–	64.6		
	Weak	δ_H	4.74	4.13	–	–	3.65	4.28	4.51	M6U
		δ_C	–	–	–	–	–	64.6		
M26	Weak	δ_H	4.93	5.48	–	–	–	4.33	4.52	–
M36	Weak	δ_H	4.83	4.20	5.09	–	–	4.31	4.53	–
G	Strong	δ_H	4.53	3.37	3.70	3.70	3.60	–	–	GU
		δ_C	103.5	74.1	75.2	79.7, 80.3	76.0	61.5		
	Weak	δ_H	4.48	3.26	3.66	–	–	–	–	GM3
		δ_C	103.5	74.3	–	–	–	–		
Gt	Strong	δ_H	4.51	3.32	3.52	3.42	–	–	–	GtU
		δ_C	103.7	74.3	76.7	70.7	–	–	–	
	Weak	δ_H	4.45	3.21	3.48	–	–	–	–	GtM3
		δ_C	–	74.5	76.7	–	–	–		

Note: "U" means "M, G, or M2". "V" means "M, G, or M3". "–" means "not assigned".
G: →4)-β-D-Glcp-(1→ residue.
Gt: non-reducing end β-D-Glcp-(1→ residue.
Mt: non-reducing end β-D-Manp-(1→ residue.
M2: →4)-2-*O*-acetyl-β-D-Manp-(1→ residue.
M3: →4)-3-*O*-acetyl-β-D-Manp-(1→ residue.
M23: →4)-2,3-di-*O*-β-D-Manp-(1→ residue.
M6: →4)-6-di-*O*-β-D-Manp-(1→ residue.
M26: →4)-2,6-di-*O*-β-D-Manp-(1→ residue.
M36: →4)-3,6-di-*O*-β-D-Manp-(1→ residue.

the TOCSY spectrum (Fig. 7). Based on the considerable difference in the chemical shifts of H-2 and H-1, the two signals sets were tentatively assigned to M6U and M6M3. ^{1}H and ^{13}C chemical shifts of residues in diads and triads, found in the current study, were summarized in Table 1.

3.5. Some discussions about the enzymatic function of mannanases

Acetylated mannoses were not found in reducing end or non-reducing end of HDOP, implying that the mannanase could not cut the glycosidic bond linked to an acetylated mannose. This explained why HDOP was rich in *O*-acetyl groups. The reducing ends of HDOP were dominantly mannoses and its non-reducing ends contained both mannoses and glucoses, indicating mannanases were capable of breaking some MM and MG diads rather than GM and GG diads. This finding was in good agreement with literature data (Schröder et al., 2001; Tenkanen et al., 1997).

3.6. $^{1}J_{C-H}$ coupling constants of major residues

$^{1}J_{C-H}$ coupling constants are important parameters relating to conformation of molecules (Maiti, Zhu, Carmichael, Serianni, & Anderson, 2006; Vuister, Delaglio, & Bax, 1993). $^{1}J_{C1-H1}$ can be

Table 2
$^{1}J_{C-H}$ coupling constants (Hz) of sugar residues and *O*-acetyl groups.

$^{1}J_{C,H}$ coupling constants	Sugar residues							*O*-acetyl groups
	M	Mt	Mα	Mβ	G	M2	M3	
$^{1}J_{C1-H1}$	161	161	170	162	158	165	162	–
$^{1}J_{C2-H2}$	153	153	–	–	146	150	–	–
$^{1}J_{C3-H3}$	146	–	–	–	–	–	–	–
$^{1}J_{Methyl\ C-H}$	–	–	–	–	–	–	–	131; 134; 135

Note: "–" means "not detected" or "not applicable for this residue or group".

used for the judgment of anomeric configuration of sugar residues (Bundle & Lemieux, 1976), based on the fact that α and β anomers of pyranoses generally give $^{1}J_{C,H}$ values of around 160 Hz and 170 Hz, respectively (Bock & Pedersen, 1974). $^{1}J_{C,H}$ coupling can be observable as doublets in HSQC or HMQC experiment without ^{13}C decoupling as well as in HMBC experiment with carefully chosen low-pass J-filters (Bubb, 2003; Duus, Gotfredsen, & Bock, 2000). $^{1}J_{C-H}$ doubles were frequently observed in previous NMR studies of glucomannans (Guo et al., 2012; Pereira et al., 2010; van Hazendonk et al., 1996). In the current study, $^{1}J_{C-H}$ coupling constants of major residues in HDOP were obtained from HMBC spectrum (Fig. 5) and were listed in Table 2. $^{1}J_{C1-H1}$ values of these residues were verified by weak doublet signals in the anomeric region of the HMQC spectrum (Fig. 4B). The pulse sequence of HMBC also enable us to obtain $^{1}J_{C-H}$ coupling constants of methyl groups in *O*-acetyl groups (Table 2), and the values were slightly lower than those in methanol reported by Maiti et al. (2006).

3.7. β-(1 → 4)-D-Galactan as contaminant

β-(1 → 4)-D-Galactan is a common component of higher plants (Mast et al., 2008), and is frequently found in some glucomannan-containing species, such as *Aloe barbadensis* (Mandal & Das, 1980), *Linum usitatissimum* (van Hazendonk et al., 1996), and Norway spruce (Hannuksela & Hervé du Penhoat, 2004). HPAEC analysis in the current study indicated the existence of minor amounts of galactoses in HDOP. A signal at 4.63 ppt in the 1D ^{1}H spectrum (Fig. 1) was assigned to →4)-β-D-Gal*p*-(1→ (designated residue g). The cross-peak at 4.63 ppm/3.67 ppm in the spectra of COSY (Fig. 2), TOCSY (Fig. 7), and NOESY (Fig. 6) was assigned to the H-1/H-2 correlation of the residue, by referring to literature data (Hannuksela & Hervé du Penhoat, 2004; van Hazendonk et al., 1996). The existence of the residue was also proved by the cross-peaks of H-1/H-3 (4.63 ppm/3.76 ppm) and H-1/H-4 (4.63 ppm/4.15 ppm) in the TOCSY spectrum. The C-1 chemical shift of the residue was extracted from the cross-peak at 105.3/4.63 ppm (C-1/H-1) in the HMQC spectrum with a low minimum contour level, and was consistent with literature data (Hannuksela & Hervé du Penhoat, 2004; van Hazendonk et al., 1996).

4. Conclusions

Majority of the *O*-acetylated mannoses in HDOP have single substitution of *O*-acetyl group at O-2 or O-3 position. Considerable amounts of mannoses were found to be *O*-acetylated at both O-2 and O-3 positions according to NMR data. This finding is the first NMR evidence for the existence of 2,3-di-*O*-acetyl-β-D-mannopyranoses in glucomannans from higher plants. Evidences for branches were not found in NMR spectra. Therefore, the major structure of Dendronan® can be shown as follows:

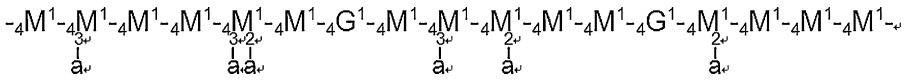

M: β-D-pyranosyl-mannose; G: β-D-pyranosyl-glucose; a: O-acetyl group

Besides, the current study is the first report of the existence of minor amounts of three mannose residues →4)-2,6-di-*O*-acetyl-β-D-Man*p*-(1→, →4)-3,6-di-*O*-acetyl-β-D-Man*p*-(1→, and →4)-6-*O*-acetyl-β-D-Man*p*-(1→ in glucomannans isolated from *Dendrobium* plants. Although the levels of these O-6 acetylated mannose residues are extremely low, their existence indicates the versatility of the *O*-acetylated mannose residues of higher plant glucomannans.

The effects of *O*-acetyl group substitution the NMR chemical shifts of ^{13}C and ^{1}H of 1,4-β-D-glucomannan were observed. Attaching an *O*-acetyl group to a ^{13}C atom in a mannose ring can increase the chemical shift of the ^{13}C atom while decrease the chemical shift of its neighbouring ^{13}C atoms in the same ring. Adding an *O*-acetyl group to a ^{1}H of a mannose residue can increase the chemical shift of the ^{1}H atom and its neighbouring ^{1}H atoms in the same mannose ring, and the closer a ^{1}H is to the newly added *O*-acetyl group, the greater the increase of its chemical shift.

Furthermore, 2-*O*-acetyl substitution of a mannose residue can increase the ^{1}H chemical shifts of the H-3 and H-5 of its neighbouring residue at the reducing end side. 3-*O*-acetyl substitution of a mannose residue can increase the ^{1}H chemical shift of H-2 of its neighbouring residue at the non-reducing end side. We designated the two effects "M2 effect" and "M3 effect", respectively. Understanding the two effects can be very helpful for researchers to interpret NMR spectra of 1,4-β-D-glucomannan from higher plants and other resources in future.

Acknowledgements

This study was financially supported by International Science & Technology Cooperation Program of China (2013DFA32710), which is gratefully acknowledged. The authors would like to thank Ms Fang Tian, president of Jin-Jiu-Di Biotechnology Co. Ltd., for providing the freeze-dried *D. officinale* stem samples and partial financial support for this study.

References

Bock, K., & Pedersen, C. (1974). A study of ^{13}CH coupling constants in hexopyranoses. *Journal of the Chemical Society, Perkin Transactions 2*, (3), 293–297.

Bubb, W. A. (2003). NMR spectroscopy in the study of carbohydrates: Characterizing the structural complexity. *Concepts in Magnetic Resonance, A*, *19A*(1), 1–19.

Bundle, D. R., & Lemieux, R. U. (1976). Determination of anomeric configuration by NMR. *Methods in Carbohydrate Chemistry*, *7*, 79–86.

Crescenzi, V., Dentini, M., Masci, G., Bernalda, M. S., Risica, D., Capitani, D., et al. (2002). A high field NMR study of the products ensuing from konjak glucomannan C(6)-oxidation followed by enzymatic C(5)-epimerization. *Biomacromolecules*, *3*(6), 1343–1352.

Duus, J. Ø., Gotfredsen, C. H., & Bock, K. (2000). Carbohydrate structural determination by NMR spectroscopy: Modern methods and limitations. *Chemical Reviews*, *100*(12), 4589–4614.

Goldberg, R., Gillou, L., & Prat, R. (1991). Structural features of the cell-wall polysaccharides of *Asparagus officinalis* seeds. *Carbohydrate Research*, *210*, 263–276.

Guo, Q., Cui, S. W., Wang, Q., Hu, X., Kang, J., & Yada, R. Y. (2012). Structural characterization of a low-molecular-weight heteropolysaccharide (glucomannan) isolated from *Artemisia sphaerocephala* Krasch. *Carbohydrate Research*, *350*, 31–39.

Hannuksela, T., & Hervé du Penhoat, C. (2004). NMR structural determination of dissolved *O*-acetylated galactoglucomannan isolated from spruce thermomechanical pulp. *Carbohydrate Research*, *339*(2), 301–312.

Hsieh, Y. S. Y., Chien, C., Liao, S. K. S., Liao, S. F., Hung, W. T., Yang, W. B., et al. (2008). Structure and bioactivity of the polysaccharides in medicinal plant *Dendrobium huoshanense*. *Bioorganic & Medicinal Chemistry*, *16*(11), 6054–6068.

Hua, Y. F., Zhang, M., Fu, C. X., Chen, Z. H., & Chan, G. Y. S. (2004). Structural characterization of a 2-*O*-acetylglucomannan from *Dendrobium officinale* stem. *Carbohydrate Research*, *339*(13), 2219–2224.

Jakes, J. E., Yelle, D. J., & Frihart, C. R. (2011). Tools to understand structural property relationships for wood cell walls. In *Italic 6—science & technology of biomass: Advances and challenges*. Viterbo, Italy: Tuscia University.

Katsuraya, K., Okuyama, K., Hatanaka, K., Oshima, R., Sato, T., & Matsuzaki, K. (2003). Constitution of konjac glucomannan: Chemical analysis and ^{13}C NMR spectroscopy. *Carbohydrate Polymers*, *53*(2), 183–189.

Ku, Y., Jansen, O., Oles, C. J., Lazar, E. Z., & Rader, J. I. (2003). Precipitation of inulins and oligoglucoses by ethanol and other solvents. *Food Chemistry*, *81*(1), 125–132.

Liu, Z. L., Peng, F., & Liu, X. G. (2012). Extraction and purification of *Asparagus oligosaccharides*. *Advanced Materials Research*, *550–553*, 1886–1892.

Lundqvist, J., Teleman, A., Junel, L., Zacchi, G., Dahlman, O., Tjerneld, F., et al. (2002). Isolation and characterization of galactoglucomannan from spruce (*Picea abies*). *Carbohydrate Polymers*, *48*(1), 29–39.

Maiti, N. C., Zhu, Y., Carmichael, I., Serianni, A. S., & Anderson, V. E. (2006). $^{1}J_{CH}$ correlates with alcohol hydrogen bond strength. *The Journal of Organic Chemistry*, *71*(7), 2878–2880.

Mandal, G., & Das, A. (1980). Structure of the D-galactan isolated from *Aloe barbadensis* Miller. *Carbohydrate Research*, *86*(2), 247–257.

Mast, S. W., Donaldson, L., Torr, K., Phillips, L., Flint, H., West, M., et al. (2008). Exploring the ultrastructural localization and biosynthesis of β(1,4)-galactan in *Pinus radiata* compression wood. *Plant Physiology*, *150*, 573–583.

Pereira, M. I., Ruthes, A. C., Carbonero, E. R., Marcon, R., Baggio, C. H., Freitas, C. S., et al. (2010). Chemical structure and selected biological properties of a glucomannan from the lichenized fungus *Heterodermia obscurata*. *Phytochemistry*, *71*(17-18), 2132–2139.

Price, N. P. J., Hartman, T. M., Faber, T. A., Vermillion, K. E., & Fahey, G. C. (2011). Galactoglucomannan oligosaccharides (GGMO) from a molasses byproduct of pine (*Pinus taeda*) fiberboard production. *Journal of Agricultural and Food Chemistry*, *59*(5), 1854–1861.

Rakhimov, D. A., Shashkov, A. S., Zhauynbaeva, K. S., Malikova, M. K., & Abdullaev, N. D. (2004). Glucomannan from *Narcissus poeticus* studied by PMR and ^{13}C NMR spectroscopy. *Chemistry of Natural Compounds*, *40*(4), 358–361.

Reynolds, W. F., & Enríquez, R. G. (2002). Choosing the best pulse sequences, acquisition parameters, postacquisition processing strategies, and probes for natural product structure elucidation by NMR spectroscopy. *Journal of Natural Products*, *65*(2), 221–244.

Roxas, M. J. T., Fukuba, H., & Mendoza, E. M. T. (1985). The absence of oligosaccharides in storage roots of sweet potato (*Ipomoea batatas* L.). *Philippine Journal of Crop Science*, *10*(3), 161–163.

Schröder, R., Nicolas, P., Vincent, S. J. F., Fischer, M., Reymond, S., & Redgwell, R. J. (2001). Purification and characterisation of a galactoglucomannan from kiwifruit (*Actinidia deliciosa*). *Carbohydrate Research*, *331*(3), 291–306.

Sen, D., Gosling, A., Stevens, G. W., Bhattacharya, P. K., Barber, A. R., Kentish, S. E., et al. (2011). Galactosyl oligosaccharide purification by ethanol precipitation. *Food Chemistry*, *128*(3), 773–777.

Swennen, K., Courtin, C. M., Van der Bruggen, B., Vandecasteele, C., & Delcour, J. A. (2005). Ultrafiltration and ethanol precipitation for isolation of arabinoxylooligosaccharides with different structures. *Carbohydrate Polymers*, *62*(3), 283–292.

Teleman, A., Nordström, M., Tenkanen, M., Jacobs, A., & Dahlman, O. (2003). Isolation and characterization of *O*-acetylated glucomannans from aspen and birch wood. *Carbohydrate Research*, *338*(6), 525–534.

Tenkanen, M., Makkonen, M., Perttula, M., Viikari, L., & Teleman, A. (1997). Action of *Trichoderma reesei* mannanase on galactoglucomannan in pine kraft pulp. *Journal of Biotechnology*, *57*(1-3), 191–204.

Thurl, S., Offermanns, J., Müller-Werner, B., & Sawatzki, G. (1991). Determination of neutral oligosaccharide fractions from human milk by gel permeation chromatography. *Journal of Chromatography B: Biomedical Sciences and Applications*, *568*(2), 291–300.

van Hazendonk, J. M., Reinerik, E. J. M., de Waard, P., & van Dam, J. E. G. (1996). Structural analysis of acetylated hemicellulose polysaccharides from fibre flax (*Linum usitatissimum* L.). *Carbohydrate Research*, *291*, 141–154.

Vuister, G., Delaglio, F., & Bax, A. (1993). The use of $^{1}J_{C\alpha H\alpha}$ coupling constants as a probe for protein backbone conformation. *Journal of Biomolecular NMR*, *3*(1), 67–80.

Xing, X. H., Cui, S. W., Nie, S. P., Phillips, G. O., Goff, H. D., & Wang, Q. (2014). Study on Dendrobium officinale O-acetyl-glucomannan (Dendronan®): Part I. extraction, purification, and partial structural characterization. *Bioactive Carbohydrate and Dietary Fibre*, *4*, 74–83.

Xu, Z. J., Lin, C. W., & Shi, Y. (2011). Isolation and structure determination of a new oligosaccharide from *Blume riparia*. *Journal of Medicinal Plants Research*, *5*(14), 2956–2962.

Zhang, L. L., Zhang, Y. Z., & Wang, L. J. (2009). Isolation of oligosaccharides from soybean molasses by alcohol precipitation. *China Oils and Fats*, *34*(4), 47–49.